Applied Radiation and Isotopes 128 (2017) 101–107

Contents lists available at ScienceDirect

Applied Radiation and Isotopes

journal homepage: www.elsevier.com/locate/apradiso

Radiosynthesis of [^{18}F]AV1451 in pharmaceutical conditions and its biological characteristics

Anne-Sophie Salabert[a,b,*], Charlotte Fontan[b], Caroline Fonta[c], Mathieu Alonso[b], Najat Loukh[a,d], Marie Bernadette Delisle[a,d], Mathieu Tafani[a,b], Pierre Payoux[a,e]

[a] "Toulouse Neuro-imaging Centre" Research Unit (UMR 1214) INSERM, Toulouse, France
[b] Radiopharmacy Department, Toulouse University Hospital, Toulouse, France
[c] Brain & Cognition Research Centre (CERCO UMR 5549), Toulouse, France
[d] Neuropathology, Toulouse University Hospital, Toulouse, France
[e] Department of Nuclear Medicine, Toulouse University Hospital, Toulouse, France

HIGHLIGHTS

- We performed radiofluorination with a pyridyl trialkyl substituted ammonium salt derivative.
- Pharmaceutical quality of [^{18}F]AV1451 was determined.
- We observed plasma protein binding of [^{18}F]AV1451.

GRAPHICAL ABSTRACT

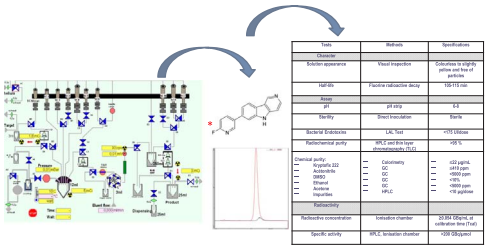

ARTICLE INFO

Keywords:
TAU protein
Radiopharmaceutical drug
Plasma protein binding
Neurodegeneration

ABSTRACT

In this study, we describe the radiosynthesis of [^{18}F]AV1451 in terms of its pharmaceutical quality and characterise its physical and biological properties. We performed an in vitro serum stability study in fresh human plasma and a plasma protein binding study. The radiochemical yield was 24% (decay corrected), and the product met all regulatory quality requirements. We found that this compound is stable in fresh human plasma and binds tightly to plasma proteins, especially lipoproteins.

1. Introduction

Alzheimer's disease (AD) is the most frequently presenting neurodegenerative diseases, affecting nearly 35 million people worldwide (James et al., 2015; Ariza et al., 2015). The diagnosis of AD can only be confirmed post mortem on the basis of the evidence of specific brain lesions. These neuropathological lesions are a combination of β-amyloid peptide deposits (APs) within plaques and hyperphosphorylated tau (tau-PHF) in neurofibrillary tangles (NFT), in neuropil threads and around amyloid deposits in neuritic plaques (Braak and Braak, 1995; Delacourte, 2006; Hardy and Selkoe, 2002; Dietmar R. Thal et al., 2002). However, over the last 10 years, biomarkers (including research on amyloid, tau and phospho-tau in the CSF) have become useful in the diagnosis of this pathology (Jack et al., 2011; McKhann et al., 2011).

Molecular imaging with positron emission tomography (PET) or single-photon emission computed tomography (SPECT) has demonstrated its ability to be a complementary technique for exploring neuronal and metabolic changes in AD. [^{18}F]fluoro-D-glucose can be used

* Correspondence to: UMR 1214 Inserm TONIC (Toulouse Neuro-imaging Centre), Université Toulouse III - Paul Sabatier, CHU PURPAN - Pavillon BAUDOT, Place du Dr Joseph Baylac, 31024 Toulouse cedex 3, France.
E-mail addresses: anne-sophie.salabert@inserm.fr (A.-S. Salabert), Fontan.Charlotte@iuct-oncopole.fr (C. Fontan), caroline.fonta@cerco.ups-tlse.fr (C. Fonta), alonso.m@chu-toulouse.fr (M. Alonso), loukh.n@chu-toulouse.fr (N. Loukh), delisle.b@chu-toulouse.fr (M.B. Delisle), tafani.m@chu-toulouse.fr (M. Tafani), payoux.p@chu-toulouse.fr (P. Payoux).

http://dx.doi.org/10.1016/j.apradiso.2017.06.032
Received 30 November 2016; Received in revised form 20 June 2017; Accepted 21 June 2017
Available online 30 June 2017

to highlight decreased glucose metabolism in hippocampal and temporoparietal cortical areas in patients, while the development of radiotracers that bind to APs has allowed for the non-invasive in vivo assessment of AD brain lesions. Several AP-selective PET radioligands have been assessed in recent years, including [^{11}C]PIB (Agdeppa et al., 2001), [^{18}F]-florbetapir (Henriksen et al., 2008), [^{18}F]-Florbetaben (Lister-James et al., 2011) and [^{18}F]-Flutemetamol (Dietmar Rudolf Thal et al., 2015).

These amyloid tracers are very useful to describe brain amyloid peptide distribution. However, amyloid deposits are known to occur without any detectable clinical symptoms.

With regard tau-PHF, Braak and Braak (Braak and Braak, 1995) have shown that the density and distribution of NFT depend on the stage of the disease, following a progressive course that ends with a major invasion of the cortex. They identified six stages correlated with cognitive dysfunction. Molecular imaging using a tracer targeting tau-PHF is a new tool for assessing the process of neurodegeneration in AD as the level of this abnormal tau is correlated with the severity of the disease (Buée et al., 2000; Delacourte, 2006; Jicha et al., 2012; Shah and Catafau, 2014).

Several PET radiopharmaceuticals have recently been developed to target abnormal tau conformations. To date, seven imaging agents have been described and are regarded as very promising TAU radioligands (Table 1).

[^{18}F]AV1451 is the same compound as [^{18}F]T807 but is referred to as [^{18}F]AV1451 throughout this publication. This compound belongs to Lilly pharmaceutical®.

[^{18}F]AV1451 binds tau-PHF with nanomolar affinity and is 25 times more selective for the tau-PHF than for Aß, proving its high specificity (Chien et al., 2013).

PET studies have shown a rapid penetration into the brain and rapid clearance in mice (Xia et al., 2013). Kidney elimination was a significant clearance pathway. Four metabolites were detected, all with a shorter retention time (RT) than [^{18}F]AV1451. In mice, 60% of [^{18}F]AV1451 remained intact 30 min after radiotracer injection (Declercq et al., 2016). To predict possible metabolism in humans, the tracer was incubated with human liver microsomes and was found to be much more stable than when incubated with mice liver microsomes (Xia et al., 2013). However, in vitro plasma stability of [^{18}F]AV1451 has not been tested on human plasma, and inter-species variability could exist. Plasma degradation could lead to the presence of metabolites causing a nonspecific signal that can damage the specificity and quality of PET imaging. To conduct quantification studies, it is important to have free fraction plasma data. This may not be a problem as long as the free fraction is constant throughout the experimental setting and the correction can be disregarded. However, it becomes a serious problem when the free fraction of the ligand in plasma is subject to change in pathological conditions (Turkheimer et al., 2015).

This article includes the description of [^{18}F]AV1451 preparation using Raytest® fluorination module and quality control of this experimental drug for human use (pre-validation run for clinical trials). In the second part, to have a better knowledge of [^{18}F]AV1451's biological properties, the lipophilicity, plasma stability and plasma protein binding of this radioligand were evaluated.

2. Materials and methods

2.1. Radiochemical synthesis

2.1.1. Reagents and apparatus

We obtained a preconditioned Sep-Pak® Light QMA cartridge with carbonate as counter ions and elution reagent (600 µL with 22 mg cryptand 222, 7 mg potassium carbonate, 300 µL acetonitrile, 300 µL water for injection) from Advanced Biomedical Compounds (ABX GmbH, Heinrich-Glaeser-Strasse 10, 14 01454 Radeberg, Germany). C_{18} Sep-Pak® Plus cartridges were obtained from Waters (Milford, MA, USA). These cartridges were then conditioned with 5 mL ethanol and 5 mL sterile water. Radioactivity was determined using a dose calibrator (Capintec® CRC-25). Automated synthesis was carried out in a Raytest® SynChrom R & D unit.

High-performance liquid chromatography (HPLC) for [^{18}F]AV1451 purification was carried out in a Raytest® synthesis module with a built-in HPLC system featuring a semi-preparative column and a C_{18} Sep-Pak precolumn. The semi-preparative HPLC was equipped with a UV detector (Knauer K-200 miniaturised UV detector) and a radioactivity detector (Raytest® Ramona star). Semi-preparative HPLC purification was conducted in a reverse column (Zorbax Eclipse XDB-C18, 9.4 × 250 mm, 5 µm). HPLC data acquisition and analysis were performed using Gina Star software.

For quality control, HPLC analysis was conducted on a modular HPLC system (Bischoff pump 3350) equipped with a reversed-phase analytic C_{18} column (4.6 × 150 mm, Luna® Phenomenex). The AV1622 (Xiong et al., 2015) and [^{19}F]AV1451 reference standards were obtained from Avid Radiopharmaceuticals (3711 Market Street, 7th Floor Philadelphia, PA 19104 phone: 215-298-0700, fax: 413-826-0416)

This HPLC system was coupled with two detectors: Detector 1 measured the radioactivity (NaI crystal, Raytest GABI detector) and Detector 2 measured the UV signal at 270 nm (ICS Lambda 1010 UV–VIS Detector). Acquisition and data analyses were performed using AQUIS® ICS software.

2.1.2. Automated synthesis of [^{18}F]AV1451

2.1.2.1. Manufacturing process. [^{18}F]$^-$ fluoride is obtained through the nuclear reaction ^{18}O (p, n) ^{18}F by the irradiation of > 97% ^{18}O-enriched water (Eurisotop®) target (2.1 mL) with a 10-MeV proton beam in an IBA 10/5 cyclotron. We typically produce on average 25 GBq per cyclotron beam for these experiments. The typical condition for irradiation was a single beam at 40 µA for 60 min. One synthesis module [^{18}F] is collected in a Sep-Pak QMA cartridge, and $H_2{}^{18}O$ is collected for recycling. A total of 600 µL eluent-reagent solution is passed through the Sep-Pak QMA cartridge, from which the trapped [^{18}F] is sent to the reaction vessel. The solvent is evaporated under helium blanketing at 115 °C. After complete removal of the solvent by azeotropic drying, the precursor AV1622 (2 mg), diluted with DMSO (1.5 mL; Dimethyl sulphoxide dried Merck 1.02931.0161), is added to the reactor vessel. The solution is heated at 110 °C for 5 min to perform the nucleophilic substitution (Fig. 1). To remove protecting groups, hydrolysis is performed with 3 N HCl solution (0.9 mL; Merck), and the mixture is heated at 100 °C for 5 min. The reaction mixture is then

Table 1
Characteristics of PHF-tau [^{18}F] radioligands: Affinity (represented by dissociation constant (Kd)), lipophilicity (represented by octanol-water partition coefficient) and information on their use (preclinical and clinical).

Compound	Kd for PHF-tau (nM)	Lipophilicity	Information
[^{18}F] FDDNP	65	3.92[16]	Lack of specificity: Kd for Aβ= 5 nM [17]
[^{18}F] THK-523	86	2.40 [18]	Lack of specificity: Kd for Aβ = 30 nM [17]
[^{18}F] THK5105	2.63	3.03 [18]	Tested on AD patients [19]
[^{18}F] THK5117	5.19	2.32 [18]	Tested on AD patients[20]
[^{18}F] AV1451 also called ([^{18}F] T-807)	14.6	1.67 [21]	Clinical trials (AD, Traumatic brain injury, etc.)
[^{11}C] PBB3	100	3.92 [22]	Lack of specificity for NFT
[^{11}C] N-methyl-lansoprazole	0.7	2.18 [23]	No fluorine derivative yet

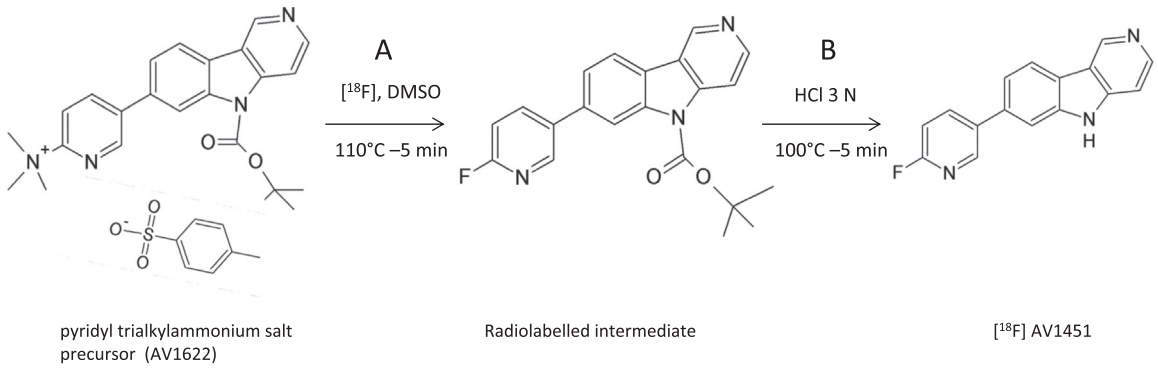

Fig. 1. Synthesis of [^{18}F]AV1451 using a radiochemistry module. A: Nucleophilic substitution in azeotropic condition in DMSO. B: Hydrolysis of BOC group with hydrochloric acid.

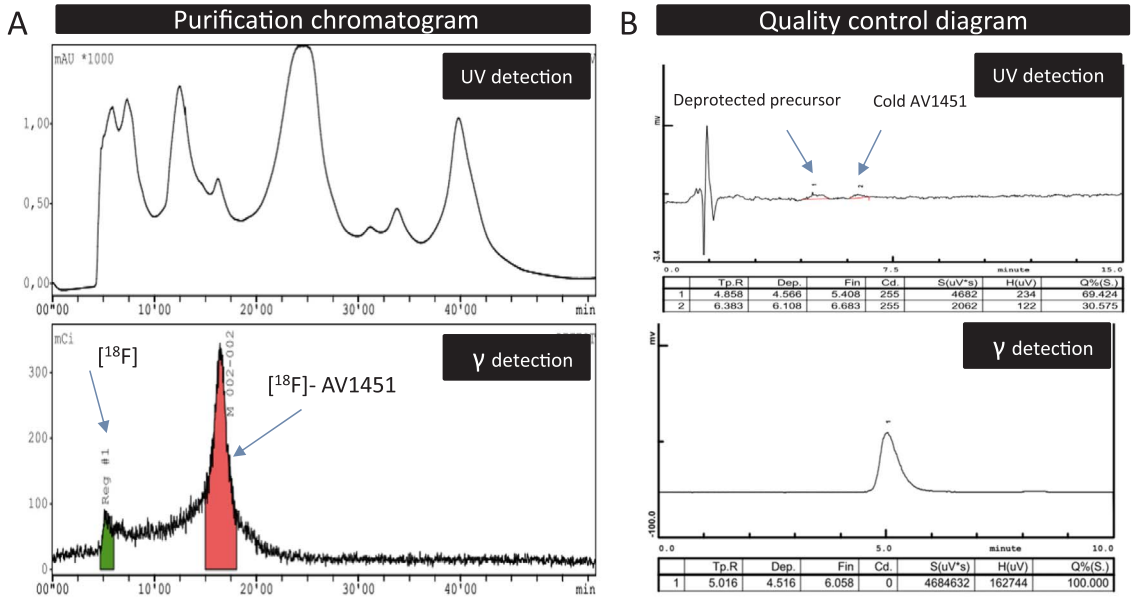

Fig. 2. A: Purification chromatogram using a semi-preparative column. Retention time of [^{18}F]-AV 1451 in the semi-preparative column was 16–18 min. B: Quality control chromotagram using an analytic column. Radiochemical purity was 99%. Cold impurities detected were cold AV1451 (0.041 ± 0.011 µg and hydrolysed AV1622 1.83 ± 1.19 µg. Amounts were calculated from internal calibration ranges. No cold AV1622 peak was detected. The total amount of these two compounds in batches did not exceed 7.11 µg.

cooled and neutralised by adding 3 N NaOH (350 µL; Cooper) and 0.5 M trisodium citrate solution (1 mL; Cooper).

The reaction mixture is trapped in a Sep-Pak C_{18} Plus and washed with 10 mL water, which removes the free fluoride. The lipophilic compound trapped in the cartridge is then eluted using 2 mL absolute ethanol. HPLC purification is performed in a semi-preparative column eluted with ethanol/sodium acetate 0.1 M (45/55) at a 2-mL/min flow rate. [^{18}F]-AV1451 RT is 16–18 min.

The fraction isolated from the HPLC purification containing [^{18}F]AV1451 is filtered in an Elumatic® flask (first filtration). Then 2 mL of this filtered solution is filtered through a 0.22-µm sterile membrane filter into a sterile vial containing 8 mL sterile saline (second filtration) to get a final concentration of ethanol less than 10%. Elumatic vials, empty, sterile pyrogen-free vials with a 15-mL capacity that are made of clear glass in accordance with the European Pharmacopoeia. These vials conform to the monography ('Glass vial for pharmaceutical use', chapter 3.2.1 of the European Pharmacopoeia). They are closed by a bromobutyl rubber stopper with an aluminium cap. The rubber stoppers are crimped on the vial with the aluminium caps. The rubber stopper and vial are provided by the Cis Bio International Company, Saclay, France.

The final solution was obtained 60 min after the start of synthesis.

2.1.3. Quality control and stability

2.1.3.1. Radiochemical purity. First, the radiochemical purity was evaluated by analytical HPLC. The final solution (20 µL) was injected onto the HPLC system. Components of the solution were separated on the HPLC column and detected by a radioactive detector. [^{18}F]AV1451 purity was determined from the ratio of the area corresponding to the [^{18}F]AV1451 peak under the sum of the area of all the detected peaks.

2.1.3.2. Identification test. Co-injection of the final product (20 µL) and cold reference [20 µL at 1 mg/mL diluted in a mixture of acetonitrile and 0.1 M sodium acetate solution (40/60)] allowed us to demonstrate that the synthesised compound corresponded to [^{18}F]AV1451. We verified that the synthesised compound and cold reference have the same RT. The mobile phase was a mixture of acetonitrile and 0.1 M sodium acetate solution (40/60). The flow rate was 1.5 mL/min, and AV1451 RT was 5–6 min.

2.1.3.3. Stability. The same experiment was repeated at T_0 + 4 h and T_0 + 6 h to verify the in vitro stability of radiolabelling.

2.1.3.4. Chemical purity. Kryptofix was detected by a comparative colour test with iodoplatinate reagent following the method described by Mock et al. (1997).

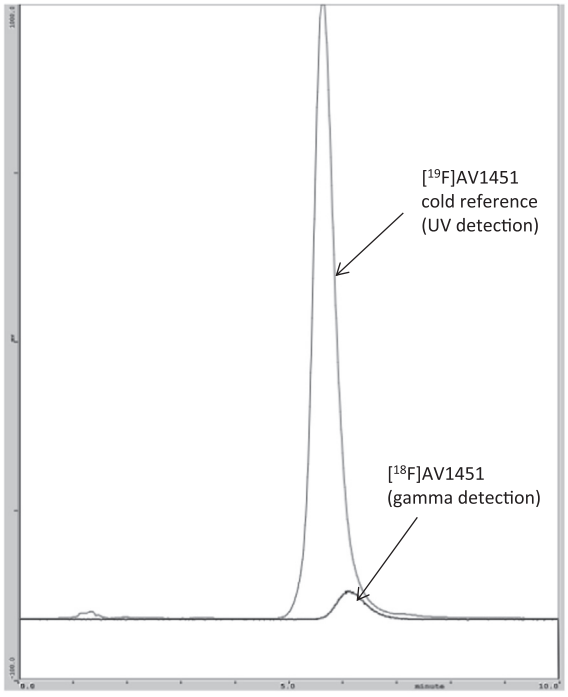

Fig. 3. HPLC traces for the confirmation of identity after co-injection of the manufactured [^{18}F]AV1451 with the cold reference [^{19}F]AV1451. (gray: UV detection; black: gamma detection).

Studies on and determination of acetonitrile, acetone, ethanol and DMSO were performed by gas chromatography following the European Pharmacopoeia for residual solvent analyses in an approved toxicology laboratory (Limoges toxicology laboratory).

Other chemical impurities can be detected by analytical HPLC (same as described in the quality control section). Qualified impurities may be calibrated against the cold reference and assayed in production batches. The first step was the injection of the formulation matrix, which showed no large interference peaks. Every possible impurity (precursor AV1622, deprotected but non-fluorinated precursor, and cold AV1451) was characterised separately to establish the RT of 8–9 min for AV1622, 3–4 min for deprotected but not fluorinated precursor, and 5–6 min for AV1451. We applied a calibration range for each of these compounds. Calibration of the model used a signal model determined by the linear least squares method without weighting. The value of the limit of detection was obtained by the approach of 3 ($xd(3\sigma) = \frac{ks0}{b}$), with k = 3, which is equivalent to that considered when a = 5%. S_0 was estimated by repetition of independent measurements of whites. Seven measures of whites allowed us to determine the limit of detection. The limit of quantification was calculated using the equation LOQ = 3.3 × LOD. For cold AV1451 and hydrolysed precursor, LODs were 0.012 and 0.009 µg, respectively, and LOQs were 0.040 and 0.030 µg, respectively.

Specific activity was calculated as activity of the sample injected in the HPLC/quantity of cold compound in the sample calculated in µmol (calculated from AV1451 cold reference calibration range).

2.1.3.5. Half-life. Calculation of the half-life provides information on the radionuclidic purity. The radioactivity of a volume of the final solution is measured using a dose calibrator at two different times. The measures of radioactivity at t1 and t2 give their corresponding activities A1 and A2. The following formula allows the calculation of the half-life, T½:T½ = ln2/(t2 – t1)/ln(A2/A1), where A1 is the first value of radioactivity measured at t1 in MBq and A2 is the second value of radioactivity measured at t2 in MBq. The result must be between 105 and 115 min.

2.1.3.6. Microbiological purity. Sterility testing was performed by the Toulouse *Institut Federatif de Biologie*. Sterility testing was conducted according to the requirements of the European Pharmacopoeia (Parenteral preparation, 07/2005, No. 0520, p. 3144–3146 and Biological test, 01/2005, No. 20601, p. 145–149). The culture was carried out on specific media for aerobic, anaerobic and mycological organisms. One millilitre of the final solution was cultured in each medium: a thioglycolate tube at 37 °C (aerobes), a trypticase soy tube at 30–35 °C (anaerobes under CO_2 atmosphere) and a fungal media tube at ambient temperature. No growth should be observed after 14 days. Control culture with PPI water was carried out following an identical method. This test is called a delayed test as the result is known after the solution has been injected into the patient.

The Limulus amoebocyte lysate (LAL) test measures the bacterial

Table 2
Quality control specifications.

Tests	Methods	Specifications	Batch 1	Batch 2	Batch 3
Character					
Solution appearence	Visual inspection	Colourless to slightly yellow and free of particles	Colourless to slightly yellow and free of particles	Colourless to slightly yellow and free of particles	Colourless to slightly yellow and free of particles
Half-life	Fluorine radioactive decay	105–115 min	110 min	111 min	110 min
Assay					
pH	pH strip	6–8	6	6	6
Sterility	Direct Inoculation	Sterile	Sterile	Sterile	Sterile
Bacterial Endotoxins	LAL Test	< 175 IU/10 mL	< 0.25 IU/mL	< 0.25 IU/mL	< 0.25 IU/mL
Radiochemical purity	HPLC	> 95%	99.967%	100%	100%
Radiochemical purity T + 6 h	HPLC	> 95%	99.187%	99.308%	99.985%
Chemical purity:					
1. Kryptofix 222	1. Colour	1. ≤22 µg/mL	1. ≤22 µg/mL	1. ≤22 µg/mL	1. ≤22 µg/mL
2. Acetonitrile	2. GC	2. ≤410 ppm	2. 32.2 ppm	2. 22.3 ppm	2. 27.6 ppm
3. DMSO	3. GC	3. < 5000 ppm	3. < 200 ppm	3. < 200 ppm	3. Not detected
4. Ethanol	4. GC	4. < 10%	4. < 7.8%	4. < 5.9%	4. 7.3%
5. Acetone	5. GC	5. < 5000 ppm	5. < 1.7 ppm	5. 4.3 ppm	5. 2.4 ppm
6. Impurities	6. HPLC	6. < 10 µg/dose	6. < 10 µg/dose	6. < 10 µg/dose	6. < 10 µg/dose
Radioactivity					
Radioactive concentration	Ionisation chamber	≥0.054 GBq/mL at calibration time (Tcal)	229 MBq/mL	135 MBq/mL	421 MBq/mL
Specific activity	HPLC. Ionisation chamber	> 200 GBq/µmol	264 GBq/µmol	426 GBq/µmol	245 GBq/µmol

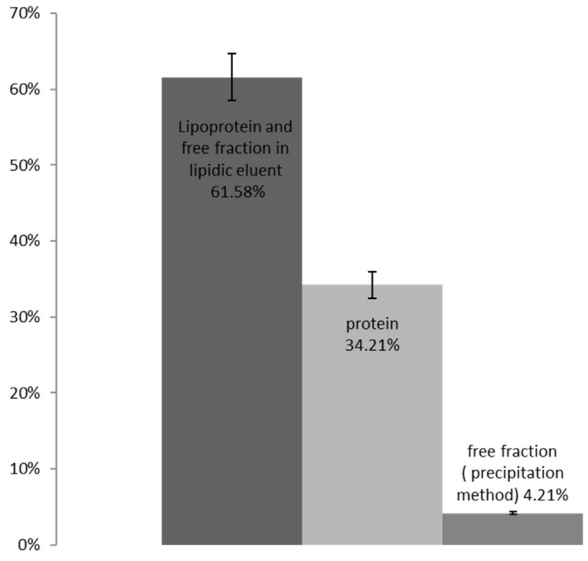

Fig. 4. Plasma protein binding of [^{18}F]AV1451 was measured in the plasma of heparinised human blood samples.

endotoxins in a solution sample. The result of the assay should be less than 17.5 IU/mL. (IU = infectious unit). In this report, the LAL test was performed by the Toulouse *Institut Federatif de Biologie*; the equipment used was Lonza QCL-1000®Limulus Amebocyte Lysate U.S.

2.2. Determination of the partition coefficient

Three samples of 30 kBq [^{18}F]AV1451 were diluted with 0.6 mL TRIS buffer (pH = 7.4) and spiked with 0.6 mL 1-octanol, vortexed for 5 min and then centrifuged at 4000 × *g* for 5 min. The layers were then separated (top: organic; bottom: aqueous) and collected in separate glass tubes. All these tubes (TRIS fraction and octanol fraction) were analysed using a Wizard gamma counter. After each count, the layers were mixed again and the processes were repeated twice. We conducted the experiment in triplicate to obtain total 18 measurements (9 buffer TRIS fractions and 9 fractions of octanol). Then we calculated logD7.4 as $LogD = Log\left(\frac{Bqof\ organic fraction - Background}{Bqof\ buffer fraction - Background}\right)$. Nine values of logD were calculated (three per sample).

2.3. In vitro serum stability test

Four samples of 500 µL fresh human plasma were incubated with 30 kBq (100 µL) [^{18}F]AV1451 at 37 °C for 10 min, 30 min, 1 h and 2 h. After incubation, the proteins were precipitated by the addition of 500 µL acetonitrile. The tubes were vortexed for 5 min and centrifuged for 10 min at 4000 × *g*. The supernatant was then injected into an HPLC column (4.6 × 250 ProntoSil C18). The isocratic mobile phase was a mixture of acetonitrile and water (60/40) and injected at a flow rate of 3 mL/min. The RT of the reference compound [^{19}F]AV1451 in those conditions was 10–11 min. Each incubation time process was repeated three times.

2.4. Plasma protein binding

The plasma protein binding of [^{18}F]AV1451 was measured in the plasma of heparinised blood samples. Plasma was prepared from fresh blood by centrifugation (15 min, 4000 × *g*) at room temperature and handled thereafter at 37 °C. Samples (800 µL) of fresh human plasma were incubated at 37 °C for 10 min, 30 min, 1 h or 2 h with 15 µL of a solution containing [^{18}F]AV1451 (30 kBq, 100 µL). The plasma was mixed with 200 µL 1-octanol, vortexed for 30 s and centrifuged for 10 min at 4115 × *g*. The 1-octanol layer was then removed and counted. The amount of radioactivity in the 1-octanol was considered the lipoprotein-bound fraction of [^{18}F]AV1451. The remaining plasma was then mixed with 200 µL acetonitrile, vortexed for 30 s and centrifuged as before. The acetonitrile layer was collected and counted. The amount of radioactivity in the acetonitrile fraction was considered the protein-bound fraction of [^{18}F]AV1451. The remaining plasma was counted, and the value obtained was considered the unbound or free fraction. Three samples were tested for each incubation time. We analysed total 12 samples. This experimentation was performed as indicated previously (Sethi et al., 2014). A control was also maintained by incubating our tracer in physiological saline to evaluate the affinity of the free fraction for the solvents used.

3. Results

3.1. Radiochemical synthesis

3.1.1. HPLC purification and yield balance

HPLC purification revealed two radioactive peaks (Fig. 2): the first one matched the free fluorine and the second one (at 16 min) corresponded to [^{18}F]AV1451. Three syntheses for batch validation were successfully performed. The radiochemical yield was 24% ± 16% (decay corrected), with a maximum yield of 37% (n = 3) and an average activity of 4316 MBq. The minimum required radioactive concentration of the solution is 54 MBq/mL at the calibration time. The recommended dosage for this drug is 240 MBq at injection time.

We can observe in Fig. 3 that the radioactive peak of AV1451 was broad. This could be because of the pH of our basic buffer (sodium acetate) that tends to retain our compound, which possesses a longer amino group. A small peak was detected in UV wavelength at the same time as the peak of [^{18}F] AV1451, and we analysed this fraction in quality control HPLC.

3.1.2. Quality control and stability

More than 99% radiochemical purity (Fig. 2B) was obtained, and the co-injection of cold reference allowed us to confirm that we produced [^{18}F]AV1451 (Fig. 3).

We observed no significant difference in radiochemical purity until 6 h after radiosynthesis.

Three analytical HPLC were performed for each batch (10 mL) to identify impurities. Average values of 0.041 µg (± 0.011 µg) for cold AV1451 and 1.83 µg (± 1.19 µg) for the hydrolysed precursor were calculated from the standard ranges. No AV1622 peak was detected. The total amount of these two compounds in batches did not exceed 7.11 µg.

The specific activity of [^{18}F]AV1451 was 312 GBq/µmol

Table 3
Comparison of radiosynthesis data obtained by using different chemical precursors.

	Shoup et al. (2013)	Chien et al. (2013)	Xia et al. (2013)	Gao et al. (2015)	Xiong et al. (2015)	Holt et al. (2016)	**Salabert et al.**
Precursor	Nitro	Nitro	Nitro	Nitro	Ammonium salt	Ammonium salt	Ammonium salt
Radiosynthesis duration	60 min	93 min	90 min	60 min	45 min	48 min	60 min
Yield (decay corrected)	20%	31%	47%	20–30%	45–55%	44%	24%
Specific activity	216 GBq/µmol	> 37 GBq/µmol	356 GBq/µmol	370 GBq/µmol	/	4.4TBq/µmol	312 GBq /µmol

(± 89 GBq/μmol).

A Kryptofix colour test determined that the concentration of these impurities never exceeded 0.22 μg/mL. The residual solvent dosage showed that the amount of these solvents met the specifications recommended by the pharmacopoeia. (Table 2)

The results of qualification tests are summarised in Table 2:

3.2. Partition coefficient

The measured distribution coefficient (logD) for [^{18}F]AV1451 was 1.088 ± 0.22 (n = 9). It is slightly lower than the log P = 1.67 observed previously by Xia et al. (Xia et al., 2013). The values were lower than the expected log P-values, 2.66 ± 0.88, calculated using ACDChemsketch® software. This is probably because this radiotracer contained ionisable groups.

3.3. In vitro serum stability test

All HPLC chromatograms contained only one peak, corresponding to [^{19}F]AV1451 RT. No degradation of AV1451 occurred within 2 h of contact between human plasma and [^{18}F]AV1451.

3.4. Plasma protein binding

As shown in Fig. 4, [^{18}F]AV1451 seemed to bind strongly to lipoprotein (62% ± 8%). This compound also bound with protein (34% ± 8%), and the free fraction was low (4.2%). AV1451 seemed to have a higher affinity for lipoproteins than for protein. The total binding fraction was 95%, so we can conclude that this tracer binds tightly to plasma proteins. This binding, tested at 10, 60 and 120 min after incubation, remained stable and close to 95% of plasma protein binding. However, in the control experiment, we observed that 54% of the activity was in the octanol fraction after incubation and centrifugation under the same conditions as that of plasma. The octanol fraction of our experiment is not only a reflection of plasma protein binding. It not only contains the bound forms but is also a part of the free fraction.

4. Discussion

We successfully synthesised [^{18}F]AV1451 using the Raytest® SynChrom module. This synthesis was reproducible, and the mean yield was 24% (decay corrected), with a maximum yield of 37%. This makes it compatible with the manufacture of doses not only for preclinical studies but also for clinical trials. The target tracer was isolated and purified by a semi-preparative HPLC combined with solid-phase extraction (SPE) in relatively high radiochemical yields, high specific activity, and radiochemical and chemical purity. In the literature, the first description of synthesis (Shoup et al., 2013) reported a 20% yield (using a *nitro* derivative as a precursor). Some other teams have recently used a pyridyl trialkyl substituted ammonium salt derivative with a good radiochemical yield (44%), as described in a previous article [19] (Holt et al., 2016). Our yield performance is not as high as those observed by Holt and Xiong et al. The Holt team used microwave heating, which could explain an increase in efficiency. The Xiong team also obtained high yields using traditional heating; however, the starting activity, the amount of precursor and the type of synthesis module used were not mentioned, which makes it difficult to compare with our results. The specific activity we observed in our manufacturing conditions was close to that reported in the literature (Table 3).

The purification method allowed us to use ethanol and 0.1 M sodium acetate solution, which is compatible with solvents for intravenous injections in humans after pharmaceutical formulation. After HPLC purification, other teams added SPE to remove any traces of acetonitrile because their HPLC semi-preparative mobile phase contained acetonitrile as the organic compound (Gao et al., 2015). Cartridges were rinsed with water and eluted with ethanol. Because SPE is time consuming, we did not follow this process and validated the safety of HPLC purification by measuring residual solvents in our batch to allow a synthesis duration of 60 min. We always observed that the concentration of acetonitrile was below the maximum standards set by the International Conference on Harmonisation.

To validate our process, we synthesised three batches, all of which underwent regulatory control steps. Quality control was essential for validating the process and ensuring the safety and quality of the manufactured product for clinical trials. Compliance with European Pharmacopoeia acceptance tests was observed.

The calculated logD was 1.1, which is slightly lower than that previously described by Xia et al. (Xia et al., 2013). This value seems to be low for a lipophilic drug, but we observed that this compound bound significantly to lipoprotein. This result is to be qualified because the extraction method does not make it possible to verify whether AV1451 is binding to plasma proteins or to the free lipophilic fraction that would have been attracted to the extraction solvent. A study on this particular octanol fraction should be conducted. However, this suggests that the plasma's lipid composition may influence the amount of radiolabelled compound present as a free fraction and therefore change its pharmacokinetics. Accordingly, there may be pharmacokinetic differences in older patients or patients with a high level of cholesterol. Further studies would be necessary to evaluate the effect of lipoprotein level and drug displacement on free fractions of [^{18}F]AV1451. In vitro stability in human serum was established (100%); metabolisation of this compound in humans does not originate from plasmatic enzymes—it was hepatic degradation that produced the metabolites described by other teams (Liang et al., 2014; Xia et al., 2013; Declercq et al., 2016).

5. Conclusion

Radiosynthesis of [^{18}F]AV1451 using a Raytest® module is reproducible, with a good radiochemical yield. This lipophilic compound tightly binds to plasma proteins. [^{18}F]AV1451 is a radiotracer whose development research is advanced, and we have developed and validated its production in the laboratory. Our production centre will be able to recruit patients and carry out new investigations on AD.

Conflict of interest statement

The authors declare that they have no competing interests.

Acknowledgments

This work has been supported in part by a grant from the French National Agency for Research called *Investissements d'Avenir* (No. ANR-11-LABX-0018-01). The authors thank Avid Radiopharmaceuticals (Eli Lilly) for providing the precursor AV1622 for Radiosynthesis and the cold reference [^{19}F]AV1451

References

Agdeppa, Eric D., Kepe, Vladimir, Liu, Jie, Flores-Torres, Samuel, Satyamurthy, Nagichettiar, Petric, Andrej, Cole, Greg M., Small, Gary W., Huang, Sung-Cheng, Barrio, et Jorge R., 2001. Binding characteristics of radiofluorinated 6-dialkylamino-2-naphthylethylidene derivatives as positron emission tomography imaging probes for β-amyloid plaques in Alzheimer's disease. J. Neurosci. 21 (24) (RC189-RC189).

Ariza, Manuela, Kolb, Hartmuth C., Moechars, Dieder, Rombouts, Frederik, Andrés, et José Ignacio, 2015. Tau positron emission tomography (PET) imaging: past, present, and future. J. Med. Chem. 58 (11), 4365–4382. http://dx.doi.org/10.1021/jm5017544.

Braak, Heiko, Braak, et Eva, 1995. Staging of alzheimer's disease-related neurofibrillary changes. Neurobiol. Aging Schmitt Symp.: Cytoskelet. Alzheimer's Dis. 16 (3), 271–278. http://dx.doi.org/10.1016/0197-4580(95)00021-6.

Buée, Luc, Bussière, Thierry, Buée-Scherrer, Valérie, Delacourte, André, Hof, et Patrick R., 2000. Tau protein isoforms, phosphorylation and role in neurodegenerative disorders1. Brain Res. Rev. 33 (1), 95–130. http://dx.doi.org/10.1016/S0165-0173(00)

00019-9.
Chien, David T., Bahri, Shadfar, Szardenings, A. Katrin, Walsh, Joseph C., Mu, Fanrong, Su, Min-Ying, Shankle, William R., Elizarov, Arkadij, Kolb, et Hartmuth C., 2013. Early clinical PET imaging results with the novel PHF-Tau radioligand [F-18]-T807. J. Alzheimer's Dis.: JAD 34 (2), 457–468. http://dx.doi.org/10.3233/JAD-122059.
Declercq, Lieven, Celen, Sofie, Lecina, Joan, Ahamed, Muneer, Tousseyn, Thomas, Moechars, Diederik, Alcazar, Jesus, et al., 2016. Comparison of new Tau PET-tracer candidates with [18F]T808 and [18F]T807. Mol. Imaging 15. http://dx.doi.org/10.1177/1536012115624920.
Delacourte, André, 2006. The natural and molecular history of alzheimer's disease. J. Alzheimer's Dis.: JAD 9 (3 Suppl), S187–S194.
Gao, Mingzhang, Wang, Min, Zheng, et Qi-Huang, 2015. Fully automated synthesis of [(18)F]T807, a PET Tau tracer for Alzheimer's disease. Bioorg. Med. Chem. Lett. 25 (15), 2953–2957. http://dx.doi.org/10.1016/j.bmcl.2015.05.035.
Hardy, John, Selkoe, et Dennis J., 2002. The amyloid hypothesis of alzheimer's disease: progress and problems on the road to therapeutics. Science 297 (5580), 353–356. http://dx.doi.org/10.1126/science.1072994.
Henriksen, Gjermund, Yousefi, Behrooz H., Drzezga, Alexander, Wester, et Hans-J.ürgen, 2008. Development and evaluation of compounds for imaging of beta-amyloid plaque by means of positron emission tomography. Eur. J. Nucl. Med. Mol. Imaging 35 (Suppl 1 (mars)), S75–S81. http://dx.doi.org/10.1007/s00259-007-0705-x.
Holt, Daniel P., Ravert, Hayden T., Dannals, et Robert F., 2016. Synthesis and quality control of [(18) F]T807 for Tau PET imaging. J. Label. Compd. Radiopharm. 59 (10), 411–415. http://dx.doi.org/10.1002/jlcr.3425.
Jack, Clifford R., Albert, Marilyn S., Knopman, David S., McKhann, Guy M., Sperling, Reisa A., Carrillo, Maria C., Thies, Bill, Phelps, et Creighton H., 2011. Introduction to the recommendations from the national institute on aging-alzheimer's association workgroups on diagnostic guidelines for alzheimer's disease. Alzheimer's Dement.: J. Alzheimer's Assoc. 7 (3), 257–262. http://dx.doi.org/10.1016/j.jalz.2011.03.004.
James, Olga G., Murali Doraiswamy, P., Borges-Neto, et Salvador, 2015. PET imaging of tau pathology in Alzheimer's disease and tauopathies. Front. Neurol. 6 (mars). http://dx.doi.org/10.3389/fneur.2015.00038.
Jicha, Gregory A., Abner, Erin L., Schmitt, Frederick A., Kryscio, Richard J., Riley, Kathryn P., Cooper, Gregory E., Stiles, Nancy, et al., 2012. Preclinical AD workgroup staging: pathological correlates and potential challenges. Neurobiol. Aging 33 (3), 622.e1–622.e16. http://dx.doi.org/10.1016/j.neurobiolaging.2011.02.018.
Liang, Steven H., Daniel, L. Yokell, Normandin, Marc D., Rice, Peter A., Jackson, Raul N., Shoup, Timothy M., Brady, Thomas J., El Fakhri, Georges, Collier, Thomas L., Vasdev, et Neil, 2014. First human use of a radiopharmaceutical prepared by continuous-flow microfluidic radiofluorination: proof of concept with the tau imaging agent [18F]T807. Mol. Imaging 13.
Lister-James, John, Pontecorvo, Michael J., Clark, Chris, Joshi, Abhinay D., Mintun, Mark A., Zhang, Wei, Lim, Nathaniel, et al., 2011. Florbetapir F-18: a histopathologically validated beta-amyloid positron emission tomography imaging agent. Semin. Nucl. Med. 41 (4), 300–304. http://dx.doi.org/10.1053/j.semnuclmed.2011.03.001.
McKhann, Guy M., Knopman, David S., Chertkow, Howard, Hyman, Bradley T., Jack, Clifford R., Kawas, Claudia H., Klunk, William E., et al., 2011. The diagnosis of dementia due to alzheimer's disease: recommendations from the national institute on aging-alzheimer's association workgroups on diagnostic guidelines for alzheimer's disease. Alzheimer's Dement.: J. Alzheimer's Assoc. 7 (3), 263–269. http://dx.doi.org/10.1016/j.jalz.2011.03.005.
Mock, Bruce H., Winkle, Wendy, Vavrek, et Michael T., 1997. A color spot test for the detection of Kryptofix 2.2.2 in [18F]FDG preparations. Nucl. Med. Biol. 24 (2), 193–195. http://dx.doi.org/10.1016/S0969-8051(96)00212-0.
Sethi, Pankaj K., Muralidhara, S., Bruckner, James V., White, et Catherine A., 2014. Measurement of plasma protein and lipoprotein binding of pyrethroids. J. Pharmacol. Toxicol. Methods 70 (1), 106–111. http://dx.doi.org/10.1016/j.vascn.2014.06.002.
Shah, Maliha, Catafau, et Ana M., 2014. Molecular imaging insights into neurodegeneration: focus on Tau PET radiotracers. J. Nucl. Med.: Off. Publ., Soc. Nucl. Med. 55 (6), 871–874. http://dx.doi.org/10.2967/jnumed.113.136069.
Shoup, Timothy M., Yokell, Daniel L., Rice, Peter A., Jackson, Raul N., Livni, Eli, Johnson, Keith A., Brady, Thomas J., Vasdev, et Neil, 2013. A concise radiosynthesis of the tau radiopharmaceutical, [^{18} F]T807: radiosynthesis of [^{18} F]T807. J. Label. Compd. Radiopharm. 56 (14), 736–740. http://dx.doi.org/10.1002/jlcr.3098.
Thal, Dietmar R., Rüb, Udo, Orantes, Mario, Braak, et Heiko, 2002. Phases of a beta-deposition in the human brain and its relevance for the development of AD. Neurology 58 (12), 1791–1800.
Thal, Dietmar Rudolf, Beach, Thomas G., Zanette, Michelle, Heurling, Kerstin, Chakrabarty, Aruna, Ismail, Azzam, Smith, Adrian P.L., Buckley, et Christopher, 2015. [(18)F]flutemetamol amyloid positron emission tomography in preclinical and symptomatic alzheimer's disease: specific detection of advanced phases of amyloid-β pathology. Alzheimer's Dement.: J. Alzheimer's Assoc. 11 (8), 975–985. http://dx.doi.org/10.1016/j.jalz.2015.05.018.
Turkheimer, Federico E., Rizzo, Gaia, Bloomfield, Peter S., Howes, Oliver, Zanotti-Fregonara, Paolo, Bertoldo, Alessandra, Veronese, et Mattia, 2015. The methodology of TSPO imaging with positron emission tomography. Biochem. Soc. Trans. 43 (4), 586–592. http://dx.doi.org/10.1042/BST20150058.
Xia, Chun-Fang, Arteaga, Janna, Chen, Gang, Gangadharmath, Umesh, Gomez, Luis F., Kasi, Dhanalakshmi, Lam, Chung, et al., 2013. [18F]T807, a novel tau positron emission tomography imaging agent for alzheimer's disease. Alzheimer's Dement. 9 (6), 666–676. http://dx.doi.org/10.1016/j.jalz.2012.11.008.
Xiong, Hui, Hoye, Adam T., Fan, Kuo-Hsien, Li, Ximin, Clemens, Jennifer, Horchler, Carey L., Lim, Nathaniel C., Attardo, et Giorgio, 2015. Facile route to 2-fluoropyridines via 2-pyridyltrialkylammonium salts prepared from pyridine N-oxides and application to (18)F-labeling. Org. Lett.. http://dx.doi.org/10.1021/acs.orglett.5b01703. (juillet).